Bioorganic & Medicinal Chemistry Letters 25 (2015) 4387–4392

Contents lists available at ScienceDirect

Bioorganic & Medicinal Chemistry Letters

journal homepage: www.elsevier.com/locate/bmcl

Discovery of novel $S1P_2$ antagonists. Part 2: Improving the profile of a series of 1,3-bis(aryloxy)benzene derivatives

Kensuke Kusumi [a,*], Koji Shinozaki [b], Yoshiyuki Yamaura [a], Ai Hashimoto [a], Haruto Kurata [a], Atsushi Naganawa [a], Hideyuki Ueda [c], Kazuhiro Otsuki [a], Takeshi Matsushita [a], Tetsuya Sekiguchi [a], Akito Kakuuchi [a], Takuya Seko [c]

[a] Minase Research Institute, Ono Pharmaceutical Co., Ltd, 3-1-1 Sakurai, Shimamoto, Mishima, Osaka 618-8585, Japan
[b] Ono Pharma UK Ltd, MidCity Place, 71 High Holborn, London WC1V 6EA, United Kingdom
[c] Head Office, Ono Pharmaceutical Co., Ltd, 8-2, Kyutaromachi 1-chome, Chuo-ku, Osaka 541-8564, Japan

ARTICLE INFO

Article history:
Received 10 July 2015
Revised 21 August 2015
Accepted 8 September 2015
Available online 8 September 2015

Keywords:
Sphingosine-1-phosphate receptor 2
Antagonist
G protein-coupled receptors
Metabolic stability

ABSTRACT

Our initial lead compound **2** was modified to improve its metabolic stability. The resulting compound **5** showed excellent metabolic stability in rat and human liver microsomes. We subsequently designed and synthesized a hybrid compound of **5** and the 1,3-bis(aryloxy) benzene derivative **1**, which was previously reported by our group to be an $S1P_2$ antagonist. This hybridization reaction gave compound **9**, which showed improved $S1P_2$ antagonist activity and good metabolic stability. The subsequent introduction of a carboxylic acid moiety into **9** resulted in **14**, which showed potent antagonist activity towards $S1P_2$ with a much smaller species difference between human $S1P_2$ and rat $S1P_2$. Compound **14** also showed good metabolic stability and an improved safety profile compared with compound **9**.

Sphingosine-1-phosphate (S1P) is a membrane-derived bioactive lysophospholipid that plays an important role in homeostasis.[1,2] S1P is present in low micromolar concentrations in plasma, and exerts most of its biological effects through five different G protein-coupled receptors (GPCRs), including $S1P_1$, $S1P_2$, $S1P_3$, $S1P_4$ and $S1P_5$.[3] $S1P_1$, $S1P_2$ and $S1P_3$ are widely expressed in a variety of tissues and cell types, whereas S1P4 and S1P5 are only expressed in a limited number of tissues. All five of these receptors are independently responsible for performing a diverse range of biological functions.[4,5]

Subnanomolar concentrations of S1P can interact with the $S1P_2$ receptor to elicit biological meaningful responses. $S1P_2$ is mainly expressed in the heart, thyroid gland, lung, trachea and liver, and it has been suggested that this receptor is involved in a broad range of important biological functions.[5]

Very few compounds have been reported in the literature to date as ligands for $S1P_2$, with CYM-5520 recently being reported as a selective agonist of this receptor.[6] JTE-013 is a well-known $S1P_2$ antagonist with an IC_{50} value in the range of 10–20 nM,[2] and numerous studies have been conducted to evaluate the biological properties of this compound.[7–10] Based on these results, it is envisaged that $S1P_2$ antagonists could become useful drugs for the treatment of various fibrotic diseases. However, there have been very few reports pertaining to the development of $S1P_2$ antagonists.

We recently reported the identification of a novel series of 1,3-bis(aryloxy)benzene derivatives as highly potent $S1P_2$ antagonists, as well as some exploration of their structure–activity relationships (SAR).[11] Compound **1** (shown in Fig. 1), which is a representative example of the compounds in this series, showed potent antagonistic activity towards $S1P_2$ (IC_{50} = 0.039 μM), as well as highbinding affinity (IC_{50} = 0.0037 μM). However, the ADME profile of **1** was unsuitable for its evaluation as a clinical candidate.

Based on these limitations, we temporarily switched our attention to an alternative lead compound and conducted another SAR study. Urea derivative **2** (shown in Table 1) was identified following the high throughput screening (HTS) of $S1P_2$ against our in-house collection of 90,000 compounds. The profile of compound **2** is shown in Table 1.

The details for this compound showed that there were three issues that would need to be solved to allow for this compound series to be developed towards a clinical candidate. The first of these issues was the difference in the antagonistic activities of compound **2** towards rat $S1P_2$ ($rS1P_2$) and human $S1P_2$ ($hS1P_2$), with the compound being 24-fold more potent towards $rS1P_2$. This

* Corresponding author. Tel.: +81 75 961 1151; fax: +81 75 962 9314.
E-mail address: kusumi@ono.co.jp (K. Kusumi).

http://dx.doi.org/10.1016/j.bmcl.2015.09.022
0960-894X/

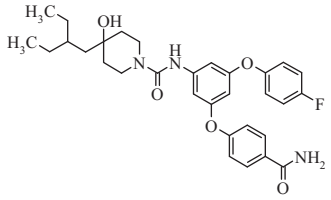

Ca^{2+} IC_{50} = 0.039 μM

Binding IC_{50} = 0.0037 μM

$logD^{a}$ = 5.11

Figure 1. Representative compound **1** from our previous report. [a]Predicted using ADMET predictor (SimulationsPlus, Lancaster, CA, USA).

Table 1
Structure and profile of lead compound **2**[12]

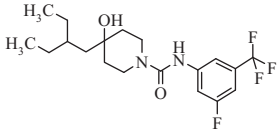

Ca^{2+} IC_{50} (μM)			Remaining ratio (%) in rat LMS, 15 min		Toxicity IC_{50} (μM)	$logD^{a}$
$hS1P_2$	$rS1P_2$	Ratio	Human	Rat		
1.7	0.072	24	40	9	37	4.78

[a] Predicted using ADMET predictor (SimulationsPlus, Lancaster, CA, USA).

difference in the species activity of the compound would have to be overcome to allow for the clinical efficacy in humans to be accurately estimated based on the efficacy in rat. The second issue with compound **2** was its poor metabolic stability in rat liver microsomes (rLMS, with NADPH, remaining ratio = 9% at 15 min.). Compound **2** also showed poor stability in human liver microsomes (hLMS, with NADPH, remaining ratio = 40% at 15 min), and these instabilities might suggest poor PK profile in both rat and human. The third issue with compound **2** was its safety profile, with the compound showing moderate levels of cellular cytotoxicity in human hepatocytes (IC_{50} = 37 μM). To develop this series towards a clinical candidate, it would therefore be necessary to overcome these three issues as well as improving the potency of this series towards $S1P_2$ through a suitable SAR study. Although this series of compounds showed lower potency than the 1,3-bis(aryloxy) benzene derivatives, we thought that compound **2** was more amenable to chemical modifications because of its low molecular weight, and modular structure.

To improve the metabolic stability of compound **2**, we initially attempted to identify the sites of its metabolism so that we could focus our efforts towards the modification of these sites to improve the stability. Unfortunately, however, our efforts in this area proved to be unsuccessful because we found a large number of oxidative metabolites in rat whole blood, which made it difficult to identify the main site of metabolism. We subsequently proceeded to investigate the metabolic 'soft-spot' of compound **2** using a chemical modification strategy. It was envisaged that the alkyl chain moiety of **2** would be preferably oxidized by cytochrome P450 enzymes to give a wide range of oxidative metabolites. To prove this hypothesis, we synthesized **3**, which had a bromophenyl moiety instead of the alkyl chain found in compound **2** and evaluated its stability in the presence of rLMS. This compound was also subjected to a rat pharmacokinetic (PK) study. Given that the urea moiety could also be a site of metabolic instability by hydroxylation, we also synthesized and tested the benzimidazole derivative **4** as a bioisostere of the urea moiety. The results for these compounds are shown in Table 2.

Compound **3** showed excellent metabolic stability in the presence of rLMS (97% @ 15 min), as well as an extremely low clearance and long half-life (CL: 0.1 ml/min/kg, $T_{1/2}$: 25 h) in the rat PK study. In contrast, the benzimidazole derivative **4** did not show enough improved metabolic stability in the presence of rLMS (47% @ 15 min) and its clearance was found to be high in rat (33 ml/min/kg) compared with compound **2**. Since compounds **3** and **4** showed close protein binding ratio (>99%), we considered that the big difference in clearances of these two compounds would be directly related to the difference of their in vitro metabolic stabilities. These results therefore indicated that the alkyl chain in compound **2** was a 'soft-spot' in terms of its metabolism and that its urea moiety was not responsible for its poor metabolic stability. Further modifications revealed that the transformation of the alkyl chain to a phenyl ring was particularly effective for improving the metabolic stability of these compounds and could therefore lead to good PK profiles.

We sometimes see that high lipophilicity would correlate to metabolic instability and/or high protein binding, and we found that compound **3** which had the least log*D* value among these compounds showed the most stable in rLMS. On the other hand, we could not see any good correlation between lipophilicity and protein binding, thus we considered that their protein binding might be too high to discuss the difference.

We also conducted an SAR study to determine whether changes to the 4-hydroxyl 4-phenyl piperidine moiety of compound **3** would be well tolerated. The results of this study are shown in Table 3.

We initially investigated the impact of changing the bromine atom on the left phenyl moiety to several other halogen atoms. Although the 4-chloro derivative **5** showed similar antagonistic activity to compound **3** (IC_{50} = 3.9 μM), the activity of the 4-fluoro derivative **6** was weaker (IC_{50} = 9.5 μM). Disappointingly, these modifications had very little impact on the metabolic stability of the compounds. Although the cytotoxicity of compound **5** was found to be slightly less than that of **3** (IC_{50} = 50 μM), with compound **6** being even less cytotoxic (IC_{50} = 69 μM). Compound **5** was ultimately selected as the best of these compounds because it was less toxic than **3** and showed better antagonistic activity than **6**. We also attempted to eliminate the hydroxyl group from compound **3** to develop a better understanding of its contribution to the activity and ADME properties of these compounds. The replacement of the hydroxyl group in **3** with a fluoride or hydrogen atom gave compounds **7** and **8**, respectively, which did not show any antagonist activity towards $S1P_2$, despite the fact that they showed excellent metabolic stability. These results therefore indicate that the hydroxyl group on the piperidine moiety is essential for the antagonistic activity of these compounds towards $S1P_2$. We observed the well-known relationship between lipophilicity and toxicity among these compounds. Lower lipophilic compounds tended to show weaker cytotoxicity. And compounds **7** and **8** which lost hydrophilic hydroxyl group showed higher log*D*s (5.30 and 5.34, respectively) and relatively potent cytotoxicities (IC_{50} = 36 and 43 μM, respectively). We considered the hydroxyl group would be worth not only achieving the antagonistic potency against $S1P_2$, but also reducing lipophilicity as well as cytotoxicity.

We previously reported the development of a novel series of highly potent $S1P_2$ antagonists,[11] and compound **1** is a representative example of the compounds belonging to this series (Table 4).

However, there were several issues associated with compound **1**. Although compound **1** showed potent antagonistic activity against $hS1P_2$ (IC_{50} = 0.039 μM), this compound also experienced similar problems to those described above for compound **2**. For example, compound **1** showed species-dependent differences in its potency (IC_{50} values of 0.039 and 0.0048 μM for $hS1P_2$ and $rS1P_2$), poor metabolic stability (24% in hLMS, 56% in rLMS) and

Table 2
Metabolic stability effects

Compd	Structure	Ca^{2+} IC_{50}(μM)			Remaining ratio (%) in rat LMS, 15 min	Rat protein binding (%)	Rat PK clearance (ml/min/kg)	log*D*[b]
		$hS1P_2$	$rS1P_2$	Ratio				
2	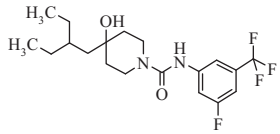	1.6	0.072	24	9.0	97	39	4.78
3	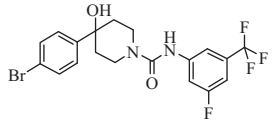	2.8	0.69	4.1	97	>99	0.1	4.47
4	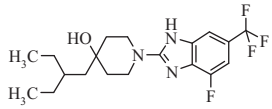	1.1	N.T.[a]	—	47	>99	33	5.28

[a] Not tested.
[b] Predicted using ADMET predictor (SimulationsPlus, Lancaster, CA, USA).

Table 3
SAR around compound **3**

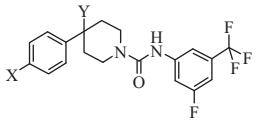

Compd	Substituent		Ca^{2+} IC_{50} (μM)			Remaining ratio (%) in LMS, 15 min		Toxicity IC_{50} (μM)	log*D*[c]
	X	Y	$hS1P_2$	$rS1P_2$	Ratio	Human	Rat		
3	Br	OH	2.8	0.69	4.1	88	97	38	4.47
5	Cl	OH	3.9	N.T.[a]	N.C.[b]	100	77	50	4.40
6	F	OH	9.5	N.T.	N.C.	97	78	69	4.10
7	Br	F	>25	N.T.	N.C.	100	100	36	5.30
8	Br	H	>25	N.T.	N.C.	100	85	43	5.34

[a] Not tested.
[b] Not calculated.
[c] Predicted using ADMET predictor (SimulationsPlus, Lancaster, CA, USA).

reasonable levels of toxicity towards human hepatocytes (IC_{50} = 29 μM). It was envisaged that the metabolic stability of **1** could be improved by changing its alkyl chain to a substituted phenyl ring in a manner similar to that described for the same modification of **2** to **5**. Based on these results, we designed and synthesized compound **9** as a hybrid compound of compounds **1** and **5**. As expected, compound **9** showed good metabolic stability in presence of human and rat live microsomes (77% in hLMS, 85% in rLMS) and potent antagonistic activities towards $hS1P_2$ (IC_{50} = 0.083 μM) and $rS1P_2$ (IC_{50} = 0.013 μM). The 4-fluoro derivative **10** showed similar potency to the 4-chloro derivative **9**, which was contrary to the results observed for compounds **5** and **6**. Furthermore, the hybrid compounds **9** and **10** showed improved species differences (6.4- and 4.5-fold, respectively) between $rS1P_2$ and $hS1P_2$ compared with **1** (8.1-fold).

Since we still observed relationship between lipophilicity and cytotoxicity, we considered that further reduction of lipophilicity would improve the safety property. Therefore we attempted to introduce polar functional groups into compound **10** to reduce its lipophilicity. Since the carboxamide moiety of **10** seemed to have chances to be changed to the other polar functional groups, we decided to focus on this position, and conducted further modifications to improve its safety profile, as well as improve the species difference in the antagonistic activity. The results of our SAR study around **10** are shown in Table 5.

Although the pyridine derivative **11** showed excellent metabolic stability (100% in hLMS, 87% in rLMS) and a slight improvement in its hepatocyte toxicity (IC_{50} = 49 μM), it gave a little bigger species difference than compound **10**. The introduction of a sulfone moiety (**12**) had only a little impact on the species difference (8.3-fold) or the metabolic stability (73% in hLMS, 85% in rLMS). Surprisingly, the cytotoxicity of compound **12** was very weak (IC_{50} > 400 μM) although the lipophilicity is higher than the others (log*D* = 4.68). The sulfonamide derivative **13** provided similar species difference (6.7-folds) and metabolic stability (72% in hLMS, 75% in rLMS) properties to compound **10**. Compound **13** also showed strong cytotoxicity towards hepatocytes (IC_{50} = 30 μM). Lastly, we synthesized the carboxylic acid derivative **14**, which gave a significant decrease in the species difference (1.9-fold) and cytotoxicity towards hepatocytes (IC_{50} = 124 μM) and increase in metabolic stability in the presence of LMS (82% in hLMS, 96% in rLMS).

Table 4
Hybrid of the two previous series

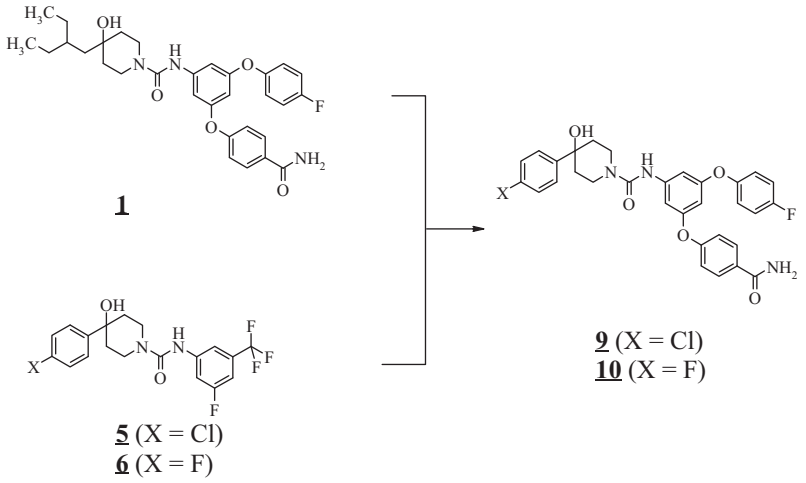

Compd	Ca^{2+} IC_{50} (μM)			Remaining ratio (%) in LMS, 15 min		Toxicity IC_{50} (μM)	log*D*[c]
	$hS1P_2$	$rS1P_2$	Ratio	Human	Rat		
1	0.039	0.0048	8.1	24	56	29	5.11
5	3.9	N.T.[a]	N.C.[b]	100	77	50	4.40
6	9.5	N.T.	N.C.	97	78	69	4.10
9	0.083	0.013	6.4	77	85	34	5.06
10	0.076	0.017	4.5	84	86	39	4.63

[a] Not tested.
[b] Not calculated.
[c] Predicted using ADMET predictor (SimulationsPlus, Lancaster, CA, USA).

Table 5
Profile of the hybrid series

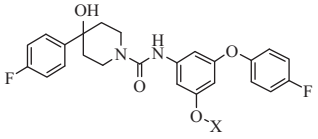

Compd	X	Ca^{2+} IC_{50} (μM)			Remaining ratio (%) in LMS, 15 min		Toxicity IC_{50} (μM)	log*D*[a]
		Human	Rat	Ratio	Human	Rat		
10	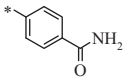	0.076	0.017	4.5	84	86	39	4.63
11		0.123	0.014	8.6	100	87	49	4.66
12	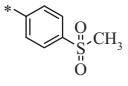	0.039	0.0046	8.3	73	85	>400	4.68
13	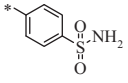	0.039	0.0058	6.7	72	75	30	4.37
14	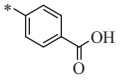	0.0062	0.0033	1.9	82	96	124	1.70

[a] Predicted using ADMET predictor (SimulationsPlus, Lancaster, CA, USA).

Table 6
Profile of compound **14**[13]

Binding assay IC_{50} (μM)				
$S1P_1$	$S1P_2$	$S1P_3$	$S1P_4$	$S1P_5$
>10	0.43	>10	>10	>10

Solubility (mg/ml) in pH 6.8 buffer	Protein binding (%)	
	Human	Rat
0.0505	99.8	99.6

Clearance in rat PK study (ml/min/kg)	Caco-2 ($\times 10^{-6}$ cm/s)	
	A–B	B–A
18	1.3	18

Based on this result, compound **14** was identified as the best compound of this series because it showed the smallest species difference in terms of its potency, as well as good metabolic stability and reduced cytotoxicity. The introduction of carboxylic acid reduced its lipophilicity dramatically ($\log D = 1.70$), which suggested its better PK and safety profiles than compound **1** had.

Additional information pertaining to the receptor selectivity and ADME profile of compound **14** was collected, and the results are shown in Table 6.

Compound **14** showed excellent selectivity against several other S1P receptors (IC_{50} values >10 μM against $S1P_1$, $S1P_3$, $S1P_4$ and $S1P_5$). Compound **14** also showed moderate solubility (0.0504 mg/ml in pH 6.8 buffer) and high protein binding (human: 99.8%, rat: 99.6%). Unfortunately, however, compound **14** did not show a sufficient improvement in rat clearance (18 ml/min/kg), despite its good metabolic stability in the rLMS assay. The relatively large clearance of the carboxylic derivative **14** was therefore attributed to it being metabolized through some conjugation pathway. It is noteworthy that compound **14** showed moderate Caco-2 permeability (1.3×10^{-6} cm/s for 'A–B' and 1.8×10^{-5} cm/s for 'B–A') with a high efflux ratio. Based on these observations, a further optimization campaign would be needed to improve the ADME properties of the series.

All of the urea derivatives described in this report were synthesized in a similar manner. A representative example of the synthetic route used for the construction of these compounds is shown in Scheme 1 for the synthesis of **14**.

Briefly, commercially available 3,5-difluoronitrobenzene (**15**) was treated with Cs_2CO_3 and 4-fluorophenol (**16**) to yield

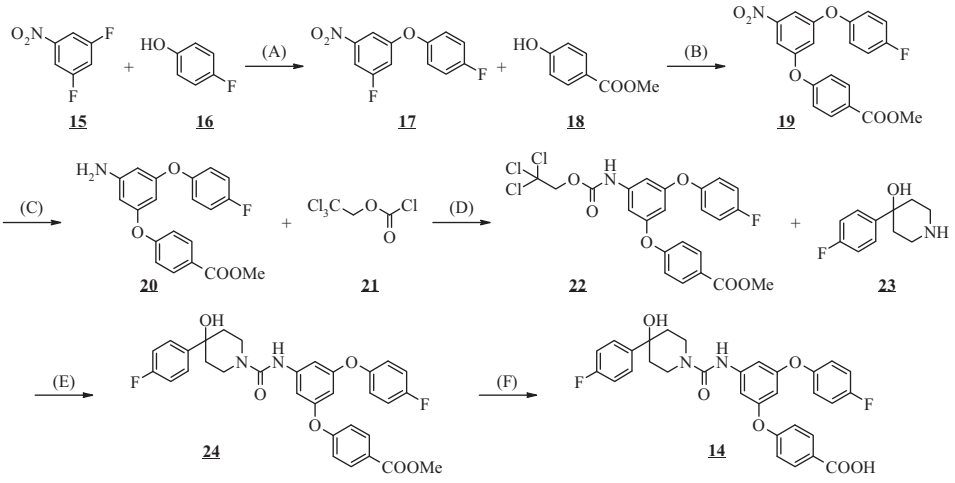

Scheme 1. Synthesis of **14**. Reagents and conditions: (A) Cs_2CO_3, DMA, 120 °C. (B) Cs_2CO_3, DMA, 120 °C. (C) H_2, 5% Pd/C, MeOH, rt. (D) $NaHCO_3$, EtOAc, rt. (E) THF, reflux. (F) 1 N NaOHaq, THF, MeOH, 40 °C.

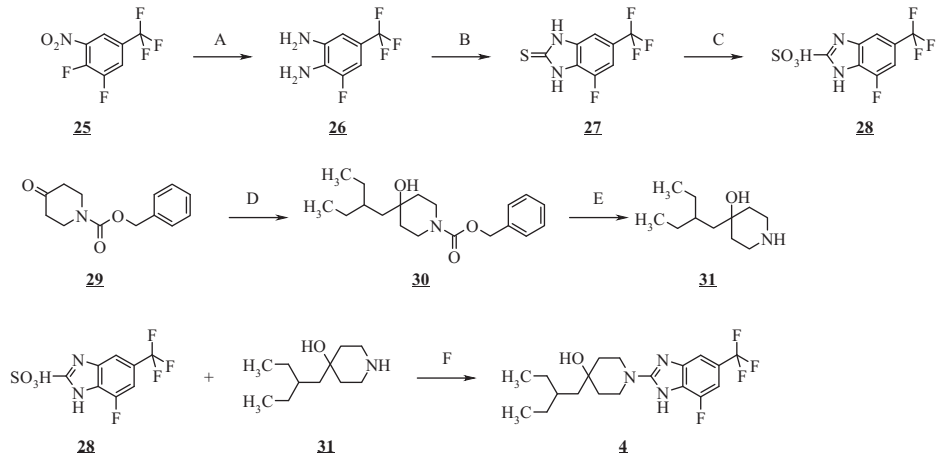

Scheme 2. Synthesis of compound **4**. Reagents and conditions: (A) NH_4OH, 1,4-dioxane, rt, then H_2, 5% Pd/C, EtOH, rt. (B) $CSCl_2$, $NaHCO_3$, CH_2Cl_2, H_2O, rt. (C) 30% H_2O_2aq, 10% NaOHaq, rt. (D) 1-Bromo-2-ethylbutane, Mg, $CeCl_3$, THF, 0 °C to rt. (E) H_2, Pd/C, EtOAc, rt. (F) Pyridine, EtOH, 150 °C microwave.

diphenylether **17**, which was subjected to a second substitution reaction using methyl 4-hydroxylphenylcarboxylate (**18**) to afford bis(aryl)ether **19**. The palladium-catalyzed hydrogenation of **19** gave aniline **20**, which was treated with 2,2,2-trichloroethyl chlorocarbamate (**21**) and $NaHCO_3$ to give intermediate **22**. The subsequent reaction of **22** with the commercially available amine **23** gave the corresponding urea **24**. The ester group of **24** was then hydrolyzed using aqueous NaOH to yield the target compound **14**.

The other compounds in Table 5 were synthesized in the same manner with **14**, using the corresponding phenol instead of **18**.

The benzimidazole derivative **4** was synthesized as according to the route shown in Scheme 2.

Common intermediate **28** was synthesized in 3 steps from a commercially available reagent. Briefly, 3,4-difluoro-5-nitrobenzotrifluoride (**25**) was treated with NH_4OH, and the resulting product hydrogenated in the presence of a palladium catalyst to afford di-aniline **26**. Compound **26** was then cyclized using thiophosgene ($CSCl_2$) to afford the cyclic thiourea **27**, which was oxidized using aqueous H_2O_2 to give sulfonic acid **28**. The other intermediate **31**, which was also used for the synthesis of compounds **1** and **11**, was synthesized in 2 steps from the commercially available N-protected piperidone **29**. Briefly, compound **29** was treated with $CeCl_3$ and 2-ethylbutane-1-yl magnesium bromide to yield alcohol **30**, which was subjected to a palladium-catalyzed hydrogenation to afford **31**. The subsequent reaction of **28** with **31** gave **4**.

Compound **2** and its derivatives in Table 3 were synthesized from the corresponding amine and 5-fluoro-3-trifluoro methyl benzene isocyanate.

In summary, we have discovered a potent and selective $S1P_2$ antagonist without species differences. The chemical modification of lead compound **2** provided the metabolically stable phenylpiperidine derivative **3**, which was combined with a bis(aryl)ether derivative to give the potent and metabolically stable $S1P_2$ antagonist **9**. Further exploration of this compound led to the introduction of carboxylic acid moiety to give **14**, which showed improved species difference and safety profile characteristics, as well as a high level of antagonist activity. Given that there are still some ADME profile issues associated with **14** (i.e., low permeability, high protein binding), further work towards the optimization of this series is currently underway in our laboratory and will be reported in due course.

Acknowledgements

The authors are deeply grateful to Dr. T. Maruyama for his many kind and helpful suggestions during the preparation of this article. The authors would also like to thank Mr. Y. Ochi for his many useful comments on this article.

Supplementary data

Supplementary data associated with this article can be found, in the online version, at http://dx.doi.org/10.1016/j.bmcl.2015.09.022. These data include MOL files and InChiKeys of the most important compounds described in this article.

References and notes

1. Blaho, Victoria A.; Timothy Hla *Chem. Rev.* **2011**, *111*, 6299.
2. Blaho, Victoria A.; Timothy Hla *J. Lipid Res.* **2014**, *55*, 1596.
3. Spiegel, S.; Milstien, S. *Biochim. Biophys. Acta* **2000**, *1484*, 107.
4. Chun, J.; Hla, T.; Lynch, K. R.; Spiegel, S.; Moolenaar, W. H. *Pharmacol. Rev.* **2010**, *62*, 579.
5. Mohamad Adadaa; Daniel Canalsa; Hannuna, Yusuf A.; Obeida, Lina M. *FEBS J.* **2013**, *280*, 6354.
6. Hideo Satsu; Schaeffer, Marie-Therese; Miguel Guerrero; Adrian Saldana; Christina Eberhart; Peter Hodder; Charmagne Cayanan; Stephan Schürer; Barun Bhhatarai; Ed Roberts; Hugh Rosen; Brown, Steven J. *Bioorg. Med. Chem.* **2013**, *21*, 5373.
7. Osada, M.; Yatomi, Y.; Ohmori, T.; Ikeda, H.; Ozaki, Y. *Biochem. Biophys. Res. Commun.* **2002**, *299*, 483.
8. Sanchez, T.; Skoura, A.; Wu, M. T.; Casserly, B.; Harrington, E. O.; Hla, T. *Arterioscler. Thromb. Vasc. Biol.* **2007**, *27*, 1312.
9. Salomone, S.; Potts, E. M.; Tyndall, S.; Ip, P. C.; Chun, J.; Brinkmann, V.; Waeber, C. *Br. J. Pharmacol.* **2008**, *153*, 140.
10. Fiorentina Roviezzo; Vincenzo Brancaleone; Luana De Gruttola; Valentina Vellecco; Mariarosaria Bucci; Bruno D'Agostino; Dianne Cooper; Raffaella Sorrentino; Mauro Perretti; Giuseppe Cirino *J. Pharmacol. Exp. Ther.* **2011**, *337*, 830.
11. Kusumi, K.; Shinozaki, K.; Kanaji, T.; Kurata, H.; Naganawa, A.; Otsuki, K.; Matsushita, T.; Sekiguchi, T.; Kakuuchi, A.; Seko, T. *Bioorg. Med. Chem. Lett.* **2015**, *25*, 1479.
12. Spectra data of **2** are shown below: ^{1}H NMR (300 MHz, $CDCl_3$) δ ppm 0.87 (t, J = 7.50 Hz, 6H) 1.06 (s, 1H) 1.38 (m, 7H) 1.64 (m, 4H) 3.34 (m, 2H) 3.84 (m, 2H) 6.59 (s, 1H) 6.96 (d, J = 8.00 Hz, 1H) 7.31 (s, 1H) 7.56 (m, 1H), ^{13}C NMR δ ppm 162.87, 153.863, 141.71, 132.47, 123.28, 111.56, 109.89, 106.66, 70.29, 46.89, 40.60, 37.14, 35.49, 27.41, 10.88.MASS: (ESI, Pos.) 781 (2M+H)+, 391 (M+H)+.
13. Spectra data of **14** are shown below: ^{1}H NMR (300 MHz, DMSO-d_6) δ ppm 8.63 (s, 1H), 7.95 (d, 2H), 7.48 (dd, 2H), 7.24 (t, 2H), 7.15–7.07 (m, 7H), 7.02 (dd, 1H), 6.31 (dd, 1H), 5.13 (s, 1H), 3.98–3.93 (m, 2H), 3.1–3.10 (m, 2H), 1.84–1.77 (m, 2H), 1.59–1.54 (m, 2H). ^{13}C NMR δ ppm 166.66, 161.80, 160.84, 160.37, 158.55, 158.40, 156.44, 154.17, 151.97, 145.60, 143.59, 131.57, 126.73, 125.61, 121.19, 117.74, 116.57, 114.41, 104.53, 103.95, 102.43, 69.65, 40.00, 37.73 MASS: (FAB, Pos.) 561 (M+H)+.